JOURNAL OF PROPULSION AND POWER
Vol. 10, No. 6, Nov.–Dec. 1994

Nonlinear Dynamic Simulation of Single- and Multispool Core Engines, Part II: Simulation, Code Validation

M. T. Schobeiri,* M. Attia,† and C. Lippke†
Texas A&M University, College Station, Texas 77843

In order to ensure the capability, accuracy, robustness, and reliability of the computational method discussed in Part I of this article, comprehensive critical performance assessment and validation tests were performed and are presented in Part II. The dynamic behavior of a subject engine is calculated by solving a number of systems of partial differential equations, which describe the unsteady behavior of the individual components. As representatives, three different transient cases with zero-, single-, and multispool thrust and power-generation engines were simulated. The transient cases range from operating with a prescribed fuel schedule, to extreme load changes, to generator and turbine shutdown.

I. Introduction

A. Simulation Test Cases

TO ensure the versatility, accuracy, robustness, and reliability of the simulation, comprehensive critical performance assessment and validation tests were performed and are presented. Table 1 shows the matrix of test cases in which the engine types, the simulation objectives, and transient types are listed.

The simulations served as the code assessment and validation using different engine configurations ranging from a zero-spool, single-shaft power-generation to a three-spool, four-shaft thrust and power-generation engine.

For code validation, the geometries of two existing power-generation gas turbine engines were employed. For code assessment purposes, different engine configurations were created and distinctive transient events were simulated. The components utilized for the different engine configurations have geometries similar to real ones.

For each engine configuration the simulation provides comprehensive information about the dynamic behavior of each component and its interaction with the other components. Since the presentation of the complete simulation results of the three cases listed in Table 1 would exceed the frame of this article, only a few selected plots will be displayed and discussed for each case.

1. Case 1: Validation, Single-Shaft CAES-Engine, Shutdown Transient

The purpose of this simulation is the validation of the presented computational method by performing a shutdown transient operation for the Compressed Air Energy Storage Plant (Huntorf, Germany) and comparing the computational results with the experiment reported by Schobeiri.[1,2]

The gas turbine system with the simulation schematic shown in Fig. 1, features predominantly the high-pressure combustion chamber CC_1, the high-pressure turbine T_1, the low-pressure combustion chamber CC_2, the low-pressure turbine T_2, the cooling-air preheater P, and the load (generator) L_1. During steady-state turbine operation, cold air from the air-storage facility, plenum 8, passes through the shutdown valve SV to the inlet plenum, where it is divided into combustion and cooling-air flows. The addition of fuel in CC_1 causes the combustion air to be heated up to the combustion chamber's exit temperature. Immediately upstream of T_1, the combustor mass flow mixes with a portion of the cooling-air flow, which has been preheated in high pressure preheater (HPP). As a result, the gas temperature of the turbine mass flow is lower than the combustion chamber's exit temperature. After expansion in T_1, the combustion chamber CC_2 mass flow is mixed in T_2 with the rest of the preheated cooling-air flow and the sealing-air flow. Immediately following expansion in T_2, the gas gives off some of its heat in P before leaving the gas turbine system.

Figure 1 shows how the various components are interconnected. Plenum 8, the air storage facility, is connected via pipe $P6$ to the shutdown valve SV. During steady-state operation, the blowoff valve BV remains closed, being opened in the event of a disturbance which might cause rapid shutdown. In such an event, the valve blows off some of the gas, thereby limiting the rotor speed. For the sake of clarity, the preheater P has been separated into its air and gas sides, designated HPP and low pressure preheater (LPP), respectively. Starting from a steady operating point, load shedding with rapid shutdown was simulated for the Huntorf turbine. Failure of the control equipment is also assumed, necessitating intervention by the hydraulic emergency system. This incident simulates an extreme transient process within some of the components, as explained briefly.

After the loss of load, the rotor is strongly accelerated because of full turbine power acting on it (Fig. 2). The hydraulic emergency system intervenes only when the speed corresponding to the hydraulic emergency overspeed trip is reached. This intervention involves closing the fuel and air valves, after which the system no longer receives any energy from outside. The total energy of the gases, still contained in the combustion chambers, is converted into mechanical energy in the turbines that follow. This process results in a steady drop in plena pressures and temperatures, with pressure shown in Fig. 3. As this figure also shows, the pressure drop in the high-pressure section (curves 1, 2, and 7) is initially steeper than in the low-pressure section. This means that the head of the high-pressure turbine is reduced more rapidly than that of the low-pressure turbine. Immediately after the blowoff valve is opened, an abrupt pressure drop takes place in plenum 10, which is connected to plenum 1 via pipe $P5$ (curve 10). Thereafter, dynamic pressure equalization takes place be-

Received April 17, 1993; presented as Paper 93-2580 at the AIAA/SAE/ASME/ASEE 29th Joint Propulsion Conference and Exhibit, Monterey, CA, June 28–30, 1993; revision received Nov. 23, 1993; accepted for publication Feb. 11, 1994.

*Professor, CFD-Propulsion Simulation Laboratory, Department of Mechanical Engineering. Member AIAA.

†Research Assistant, CFD-Propulsion Simulation Laboratory, Department of Mechanical Engineering.

Table 1 Matrix of simulation cases

Test	Engine type	Test objective	Test type
Case 1	Power-generation gas turbine engine, single shaft, two turbines, two combustors, BBC CAES	Code validation, rotor speed test	Generator and turbine shutdown
Case 2	Power-generation gas turbine engine, single spool, single shaft, BBC-GT9	Code validation and performance test and assessment	Adverse load changes
Case 3	Thrust and power-generation core engine, three spool, four shafts	Code performance, assessment, and test	Operation with fuel schedule

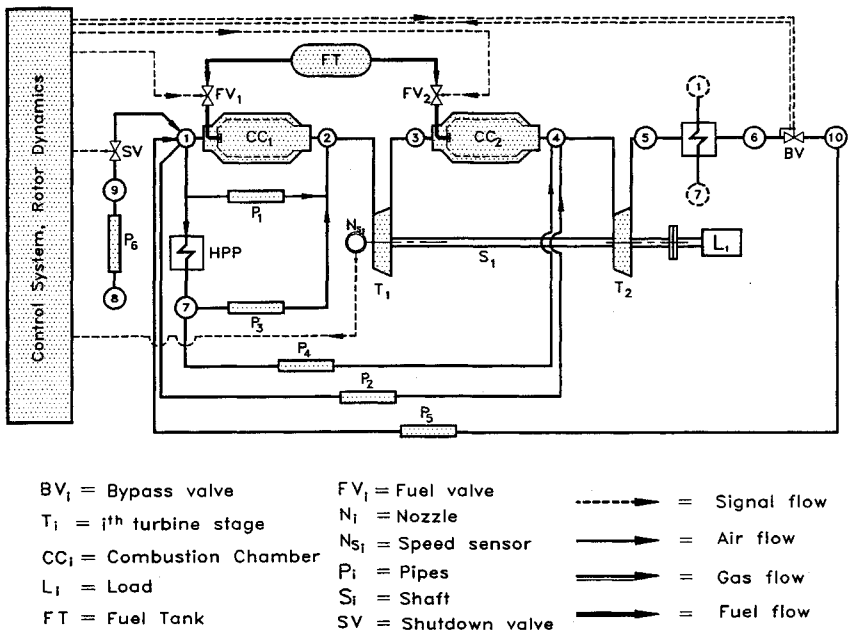

Fig. 1 Simulation schematic for a zero-spool, single-shaft engine, case 1.

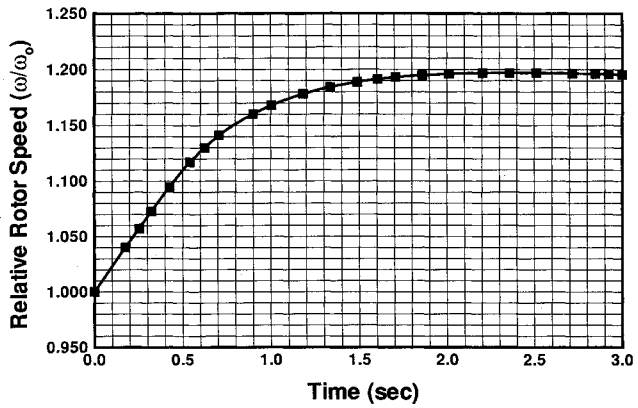

Fig. 2 Relative rotor speed as a function of time, case 1.

tween the two plena. For greater clarity, the insert plot of Fig. 3 shows an enlargement of the sharp pressure change. The plotted pressure transients for the plena 1, 2, 7, and 10 demonstrate the situation mentioned above. The results of the calculation and measurement agree well over a wide range. This dramatic drop in pressure and temperature necessitates a corresponding drop in the mass flow throughout the engine. Figure 4 characterizes the mass flow through both turbines as representatives for the entire engine. Figure 5 shows the resulting drop in turbine power.

The dynamic behavior of the rotor speed is generally determined by the turbine power acting on the rotor. How the rotor behaves in response to loss of load depends, in particular, on how long the full turbine power is available—a process monitored by the control and protection system. When the control system functions perfectly, load shedding is signaled without delay to the valve. Failure of the control system causes the hydraulic emergency system to intervene. In the following, only the second case is examined. The intervention begins only when the speed corresponding to the hydraulic emergency overspeed trip is reached. During this process, and also the subsequent valve dead-time, the rotor receives the full turbine power. The closing phase is characterized by a steady reduction in energy input from outside, which finally becomes zero. The total energy of the gases still contained in the system is converted by the two turbines into mechanical energy, causing the rotor speed to increase steadily (Fig. 2). When the instantaneous turbine power is just capable of balancing the friction and ventilation losses, the rotor speed reaches its maximum, not to exceed the overspeed limit, after which it begins to decrease (Fig. 2). Close agreement between the computed rotational speed for this critical case and the experimental measurements is also demonstrated in Fig. 2.

2. Case 2: Validation, Single-Spool, Single-Shaft Engine

The purpose of this simulation was to validate the versatile simulation capability of the presented computational method by performing an adverse transient operation and comparing the computational results with experimental measurements. The BBC-GT9 gas turbine engine was chosen for this test. Experimental data of this engine and this transient operation were documented by Schobeiri.[2,3]

The engine under consideration is shown in Fig. 6 with its schematic representation. It consists of a 15-stage compressor which could be divided into three groups; low-pressure, intermediate pressure, and a high-pressure compressor. A com-

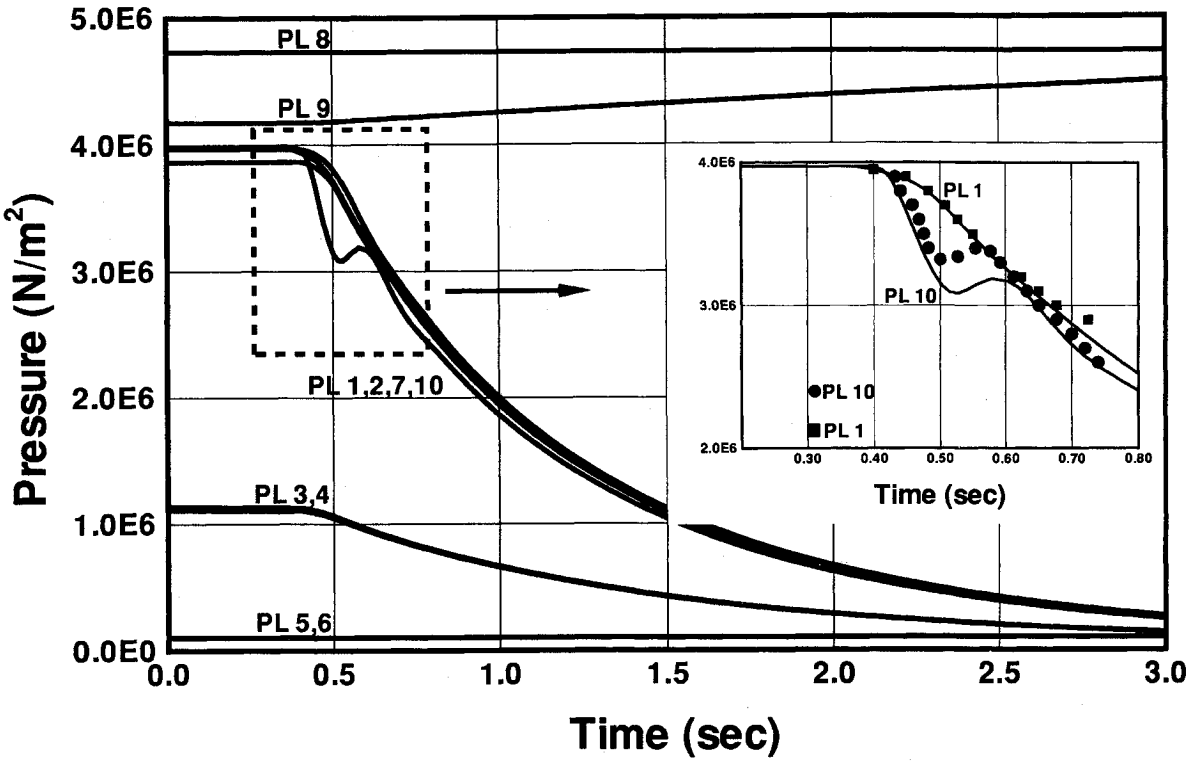

Fig. 3 Plena pressures as functions of time, case 1.

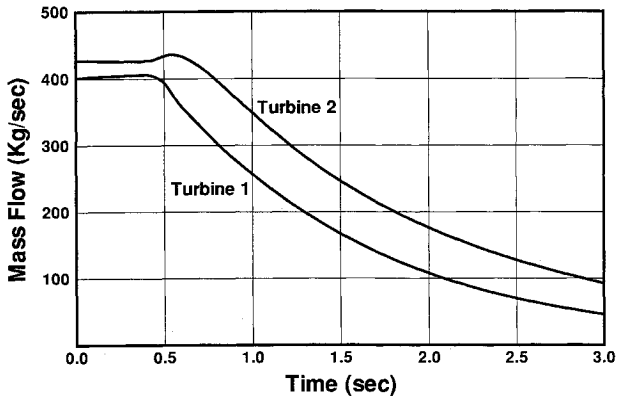

Fig. 4 Turbine mass flows as functions of time, case 1.

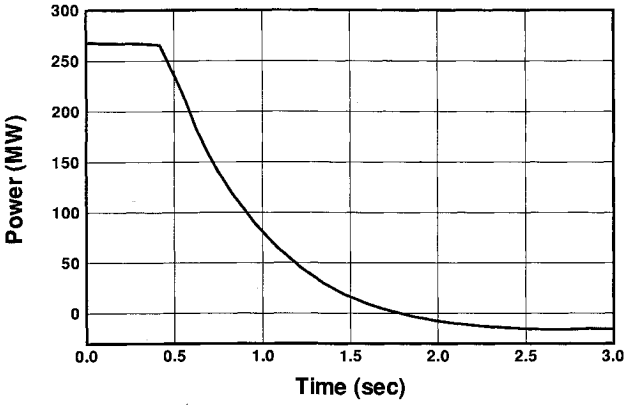

Fig. 5 Gas turbine power output as a function of time, case 1.

bustion chamber is followed by a four-stage turbine, and a generator. The rotor speed and the turbine inlet temperature are the input parameters to the control system. The output is the fuel mass flow, which governs the behavior of the engine during this transient operation.

Starting from steady-state operation, as shown by Fig. 7, curve (1), a total generator loss of load is simulated. The rotor reacts with a corresponding increase in rotational speed (Fig. 8). This increase in rotational speed triggers a rapid closing of the fuel valve, as shown by the fuel mass flow plot insertion of Fig. 9. The rotational speed is then brought to an equilibrium and held approximately constant. This event is followed by a sudden addition of load, and a gradual loss such that the engine is supplying approximately 25% of its rated load (Fig. 7). The turbine and compressor components are quick to sense the increase in the shaft rotational speed, resulting in an increase in the mass flow through the engine (Fig. 9). The mass flow continues to react according to the changes in rotational speed. It is worth noting, when comparing the turbine mass flow to that of the compressor component, that the mass flow through the turbine seems to be reacting more intensely to this transient. This behavior is justified by the fact that the turbine component is directly downstream from the combus-

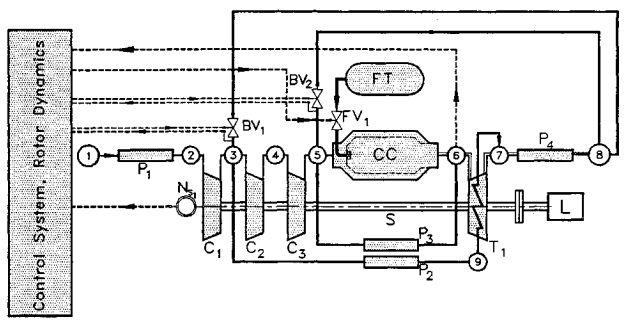

Fig. 6 Simulation schematic of a single-spool, single-shaft engine, case 2.

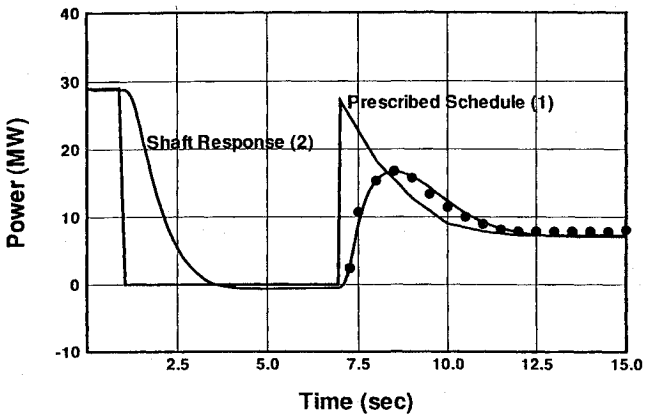

Fig. 7 Gas turbine power output as a function of time, case 2.

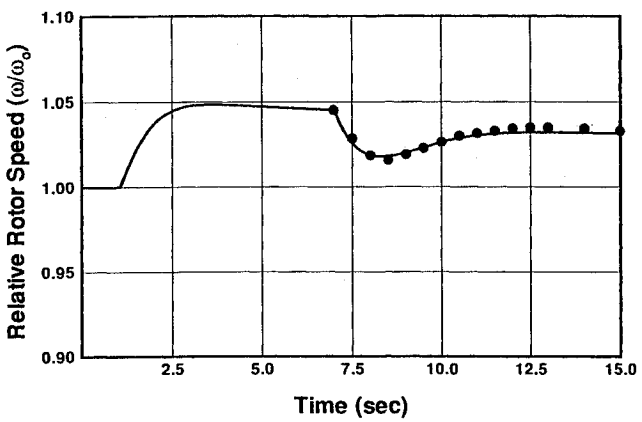

Fig. 8 Relative rotor speed as a function of time, case 2.

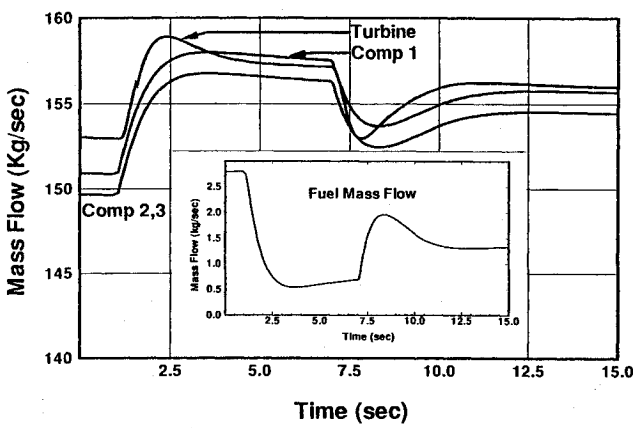

Fig. 9 Turbine, compressor, and fuel mass flows as functions of time, case 2.

tion chamber. On the other hand, the compressor, which is upstream of the combustion chamber, develops a less intense reaction to the sharp drop of fuel mass flow (Fig. 9).

B. Comparison Between Measurements and Calculations

The results of the above simulation were compared with experimental data for the same transient, documented by Schobeiri.[2,3] Although the measurements of pressure and particularly temperature may be subject to a certain amount of inaccuracy, those of power and rotational speed can be directly obtained without any major error. The experimental measurements of Figs. 7 and 8 show close agreement with the computational results.

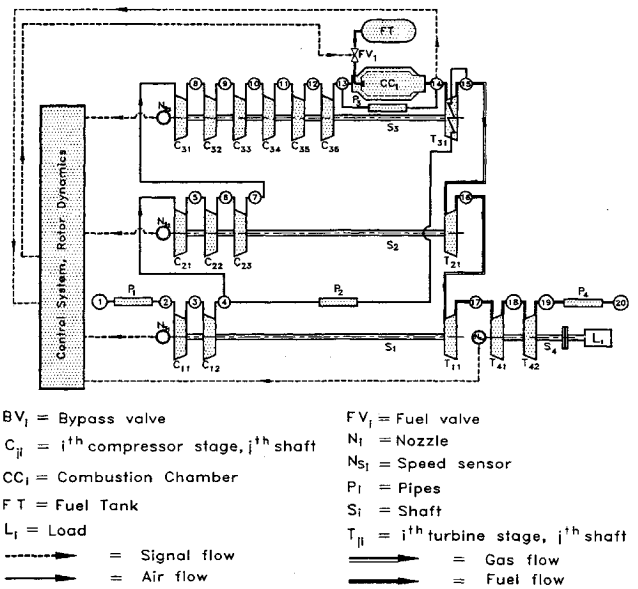

Fig. 10 Simulation schematic of a three-spool, four-shaft engine, case 3.

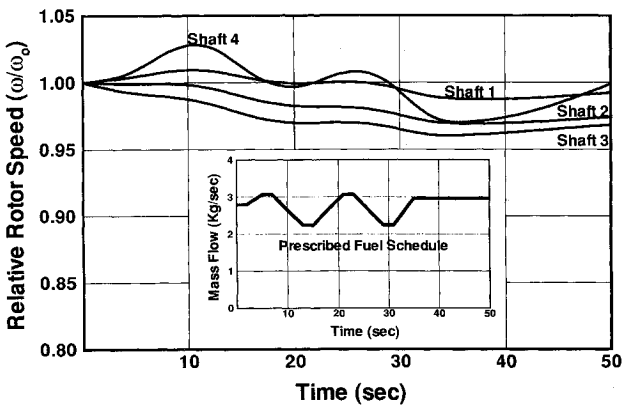

Fig. 11 Relative rotor speed and prescribed fuel schedule as functions of time, case 3.

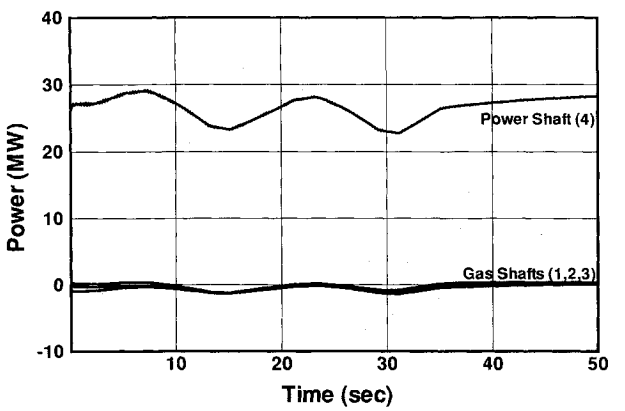

Fig. 12 Gas turbine power output as a function of time, case 3.

3. *Case 3: Adverse Transient, Three-Spool, Four-Shaft Engine*

After simulation of the above single-spool engines was successfully completed, a decision was made to simulate a more complex engine. For this purpose a three-spool thrust generating engine was designed. To increase the level of complexity, a fourth shaft S_4, with the power generating turbine T_4 was attached to the exit of the three-spool gas generating

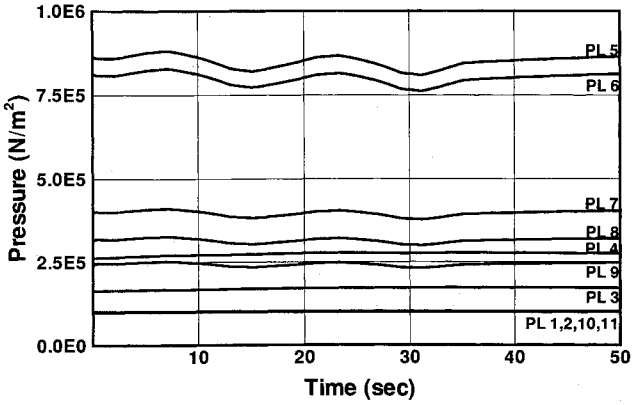

Fig. 13 Plena pressures as functions of time, case 3.

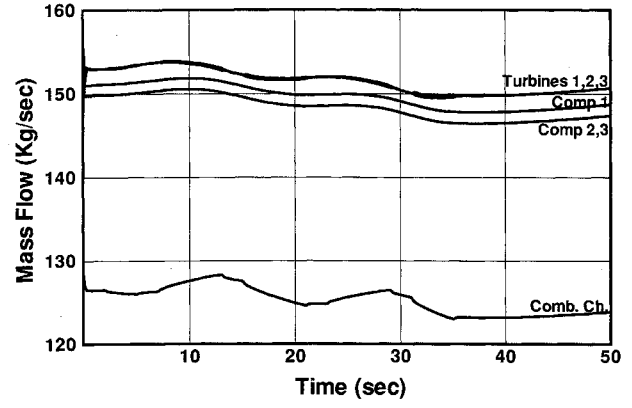

Fig. 14 Turbine, compressor, and combustion chamber mass flows as functions of time, case 3.

unit as shown in the schematic of Fig. 10. The scheme of this transient operation is fully governed by a prescribed, oscillating fuel schedule. The component nomenclature for this configuration is the same as for the previous cases.

Starting from steady-state operation, the dynamic behavior of the above engine is simulated for a transient operation that is controlled by the fuel schedule shown as an insert in Fig. 11. The power shaft, curve (4), Fig. 11, reacts to this event with a corresponding change in rotational speed. The resulting turbine power outputs are shown in Fig. 12. The change in fuel mass flow triggers a corresponding change in temperature and pressure in the various plena, with pressure variations shown in Fig. 13. The mass flow through the engine was also affected by this transient, as shown in Fig. 14.

II. Conclusions

To ensure the capability, accuracy, robustness, and reliability of the computational method discussed in part I of this article, three critical performance assessment and validation tests were performed by simulating adverse transients for single-spool single-shaft, and three-spool four-shaft power-generation, and thrust/power-generation engines. For the code validation, the geometries of two existing engines, a single-spool power-generation gas turbine engine (BBC-GT9) and a zero-spool, single-shaft high-pressure compressed air energy storage facility, were employed. For code assessment purposes, different engine configurations were created and distinctive transient events were simulated. The computational results have shown that the presented method is capable of simulating complex engine configurations with accurate and realistic results, regardless of the type of the engine, number of components, spools, or shafts. Adverse transients were simulated, and the high degree of agreement between the above results and the experimental data is the first indication of the high prediction accuracy of the presented computational method.

Acknowledgments

The authors would like to express their sincere thanks and appreciation to Carl Lorenzo, Chief System Dynamics Branch, Dan Paxson, and the administration of the NASA Lewis Research Center for the continuous cooperation and support of this project.

References

[1]Schobeiri, H., and Haselbacher, H., "Transient Analysis of Gas Turbine Power Plants Using the Huntorf Compressed Air Storage Plant as an Example," American Society of Mechanical Engineers, ASME-85-GT-197, 1985.

[2]Schobeiri, T., "Digital Computer Simulation of the Dynamic Operating Behavior of Gas Turbines," *Journal Brown Boveri Review 3-87*, 1987, pp. 161–173.

[3]Schobeiri, T., "A General Computational Method for Simulation and Prediction of Transient Behavior of Gas Turbines," American Society of Mechanical Engineers, ASME-86-GT-180, 1986.